First-principles investigations of the electronic, optical and chemical bonding properties of SnO_2

Ph. Barbarat,[a] S. F. Matar[b] and G. Le Blevennec[a]

[a]*CEA Le Ripault, Département Matériaux, 37260 Monts, France*
[b]*Institut de Chimie de la Matière Condensée de Bordeaux—CNRS, Chateau Brivazac, Avenue du Docteur Schweitzer, F-33608 Pessac, France*

The electronic structure of the rutile-type oxide SnO_2 is examined self-consistently using the augmented-spherical-wave (ASW) method within the density-functional theory (DFT). The influence of hybridization between the different l-states on the chemical bonding is discussed from the density-of-states (DOS) and the crystal orbital overlap population (COOP) results. A description of the nature of chemical bonding in SnO_2 is provided along with the investigation of the optical properties. An overall agreement was found between the calculated and the experimental optical properties in the UV spectrum.

The purpose of this work is to present and discuss the intrinsic electronic, optical and chemical bonding properties of SnO_2 calculated self-consistently by means of the augmented-spherical-wave (ASW) method within the density-functional theory (DFT). The properties of metal oxides have received a great deal of interest for many years, due to many fields of application such as solar cells, optical devices and oxidation catalysts, in the particular case of SnO_2. Even though these applications are often related to the extrinsic behaviour of stannic oxide, a detailed understanding of the fundamental electronic structure and properties is required to obtain high-quality materials. Theoretical studies and DFT calculations especially were found to provide valuable information about the electronic or the UV optical properties of rutile-type oxides ranging from CrO_2,[1,2] the only ferromagnetic half-metallic rutile oxide at room temperature, to insulating oxides such as TiO_2.[3,4] Concerning SnO_2, Jacquemin *et al.*[5,6] used the Kohn–Korringa–Rostoker (KKR) method along with semi-empirical potential models to study the optical transitions related to the minimum band gap. A similar investigation was carried out by Arlinghaus[7] using a self-consistent augmented-plane-wave (APW) method and Robertson[8] reported the SnO_2 band structure derived from a tight-binding method with scaled two-centre interactions. Svane and Antoncik[9] investigated the SnO_2 band structure and the charge distribution within the crystal using the linear muffin-tin-orbital (LMTO) method. More recently, extrinsic properties of SnO_2 such as dopant and surface reduction effects have been studied within the framework of DFT.[10,11] However additional calculations are needed in order to acquire a deeper understanding of the intrinsic optical and chemical bonding properties of SnO_2. Therefore we provide here a theoretical study of the electronic structure of SnO_2 that leads to a description of both the nature of chemical bonding and the character of the optical behaviour in the UV spectrum. This paper is organized as follows: the calculational method is first presented followed by the description of the crystal structure used in this work. The band structure and density-of-states results are then discussed followed by the crystal-orbital-overlap-population analysis. The calculated UV absorption spectrum is presented and compared with experiment. Finally, a brief conclusion is provided.

Calculational method

As in our earlier studies of oxide systems[2,12] we use the augmented-spherical-wave (ASW) method[13] to calculate the electronic properties of SnO_2. In the limited ASW basis set,[13] the chosen valence partial wavefunctions for the different species are as follows: Sn (5s,5p), O (2s,2p), *i.e.* $l_{max}=1$ for tin and oxygen respectively, l being the secondary quantum number. The ASW method is based on the density-functional theory (DFT)[14] which accounts for the ground state properties of a compound, *i.e.* the calculations are carried out at $T=0$ K. The effects of exchange and correlation are treated within the local-density approximation (LDA) using the parametrization scheme of von Barth and Hedin[15] and Janak.[16] This locality provided by the LDA to the DFT gives the labeling of local-density functional (LDF) to the calculations.

Within the atomic sphere approximation (ASA), the ASW method assumes overlapping spheres centered on the atomic sites whose volume has to be equal to the cell volume. Within the spheres the potential has a spherical symmetry, *i.e.* central potential. As the rutile structure is not closely packed, empty spheres (ES) are introduced to represent the interstitial space and to avoid an otherwise too large overlap between the actual atomic spheres of Sn and O. ES are pseudo atoms with zero atomic number. They receive charges from the neighboring atomic species and allow for possible covalency effects within the lattice.

The Brillouin zone (BZ) integration was carried out for 825 k-points in the irreducible wedge. Self-consistency was obtained when no variation of the charge transfers ($\Delta Q<10^{-6}$) and of the total variational energy E_{var} ($\Delta E<10^{-6}$ Rydberg) could be observed upon additional cycles.

Furthermore in this work chemical bonding features are discussed based on the crystal orbital overlap population (COOP) initially developed by Hoffmann from the quantum chemistry standpoint (extended Hückel calculations).[17] This allows for the density-of-states (DOS) features to be assessed on the basis of chemical bonding criteria which in a lax notation consists of weighting the DOS with the sign and magnitude of the overlap integral between the relevant orbitals.

The optical absorption spectrum is calculated as the real part of the frequency-dependent interband optical conductivity in the dipole approximation evaluated with the Kubo formula.[18,19]

Crystal structure

SnO_2 exhibits the rutile structure with space group $P4/mnm$. The unit cell is simple tetragonal and contains six atoms, two tin and four oxygen. Atomic positions are determined by the

c/a ratio and the internal parameter u.[20] The cations are at (0,0,0) and $(\frac{1}{2},\frac{1}{2},\frac{1}{2})$ and are surrounded by a distorted octahedron of anions at $\pm(u,u,0)$ and $\pm(\frac{1}{2}+u,\frac{1}{2}-u,\frac{1}{2})$. Each cation has two anions at a distance of $\sqrt{2}ua$ and four anions at $[2(\frac{1}{2}-u)^2+(c/2a)^2]^{\frac{1}{2}}a$. Each anion is found to be bonded to the cations in a planar-trigonal configuration in such a way that the oxygen p orbitals contained in the four-atom plane, *i.e.* p_x and p_y orbitals, define the bonding plane. Consequently, the oxygen p orbitals perpendicular to the bonding plane, *i.e.* p_z orbitals, have a non-bonding character and are expected to form the upper valence levels. In the work presented here, values of 4.737, 3.186 Å and 0.307 are used for a, c and u parameters, respectively.[20] Our non-unique choice of the atomic sphere radii which minimize the overlap between the atomic spheres was subjected to the following ratios: $r_{Sn}/r_O = 0.875$, $r_O/r_{ES1} = 1.333$, $r_{ES1}/r_{ES2} = 1.089$, where ES1 and ES2 are empty spheres placed at $(0,\frac{1}{2},\frac{1}{4})$ and $(u,-u,0)$, respectively. Since the minimum band gap value was found to be rather sensitive to the sphere radii, our choice for the atomic sphere radii was determined in order to reproduce the experimental minimum band gap value.

Results and Discussion

Band structure and density-of-states results

The calculated band structure of SnO_2 along the symmetry lines of the simple tetragonal Bravais lattice is shown in Fig. 1, where the Fermi level is chosen to be the zero of the energy scale.

A basic feature of the band structure presented here is that the maximum of the valence band is located at the R-point of the BZ whereas the minimum of the conduction band is at Γ. Therefore, the lowest-energy optical transition is found to be a R→Γ phonon-aided indirect transition as reported in other theoretical studies.[7,9] This result is inconsistent with experiment since the SnO_2 minimum band gap is believed to correspond to a direct dipole-forbidden transition at the Γ-point.[9] The experimental minimum band gap magnitude varies from 2.25 to 4.3 eV, depending on the sample purity.[6,21] However a reasonable value for the SnO_2 minimum band gap at 0 °K would be within the range 3.6–3.9 eV.[6,22,23] In our calculations the energy difference associated with the R→Γ indirect transition is *ca.* 3.6 eV and the lowest energy direct interband transition, *i.e.* the minimum direct gap, is a Γ→Γ transition of *ca.* 4.0 eV.

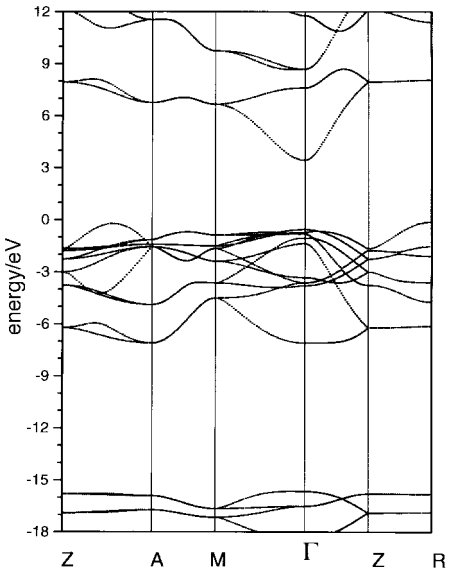

Fig. 1 Band structure of SnO_2

Another relevant feature of the band structure is the free-electron-like character of the conduction band in the Γ–Z and Γ–M directions, as reported in other studies.[7,8,10]

Moreover, a theoretical valence band width of *ca.* 7.5 eV is found, the experimental value being 9–10 eV.[21,24,25] As presented in Fig. 2(*b*), the SnO_2 valence band features obtained from our calculations are seen to be in agreement with UV photoelectron spectroscopy (UPS) measurements.[21]

The projection of the DOS for the l-states for each one of the two constituent species is presented in Fig. 2(*a*) and (*b*). A large contribution of Sn(s)-states is found at the bottom of the valence band between −7 and −5 eV. Then from −5 eV to the top of the valence band, the Sn(p)-states contribution is decreasing as the Sn(d)-states contribution is increasing. The Sn(d)-states are found to occupy the top of the valence band. A large and extended contribution of O(p)-states is found in the valence band. Clearly, bonding between Sn and O is predominated by the p-states of the latter. The projection along the Cartesian axes showed equal contribution from in-plane p_x and p_y orbitals and slightly different shape of $O(p_z)$ ones which are characterized by a very sharp peak close to the top of the valence band as expected from crystal structure considerations. The conduction band shows a predominant contribution of Sn(s)-states up to 9 eV. Then, for energies larger than 9 eV, an equal contribution of Sn- and O-states is found in the conduction band.

Crystal orbital overlap population results

The interatomic interaction can be further investigated by examining the COOP. As described above, in the rutile structure the metal is in a non-regular octahedron of oxygen atoms and SnO_6 octahedra are edge sharing. Because of this feature of stacking octahedra there could exist non-negligible O—O interactions beside the Sn—O ones. This we illustrate by showing the relevant COOP in following figures where positive, negative and zero values along the y-axis are relative to bonding, antibonding and non-bonding interactions respectively. Beside the COOP given for two-body interactions for all the valence basis set, we give a projection as well for p and d orbitals for each atomic species in order to address their respective roles.

Fig. 3(*a*) shows the COOP for the Sn—O and O—O interactions for one atom of each species. They are clearly dominated by both kinds of interactions. The energy range where Sn(p)-states predominate (−4 to −2 eV) shows bonding features of Sn—O interaction which then becomes antibonding. There are concomitantly bonding and antibonding O—O

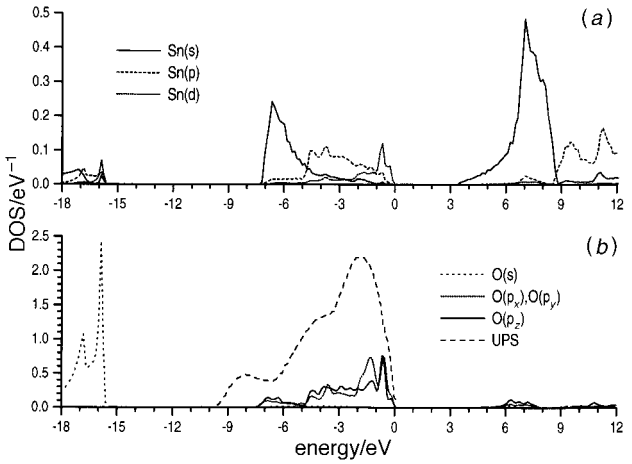

Fig. 2 Partial density-of-states (DOS) for SnO_2: l-projected DOS for tin (*a*); l- and Cartesian-projected DOS for oxygen (*b*); also shown in (*b*) are the UV photoelectron spectroscopy (UPS) measurements from ref. 21

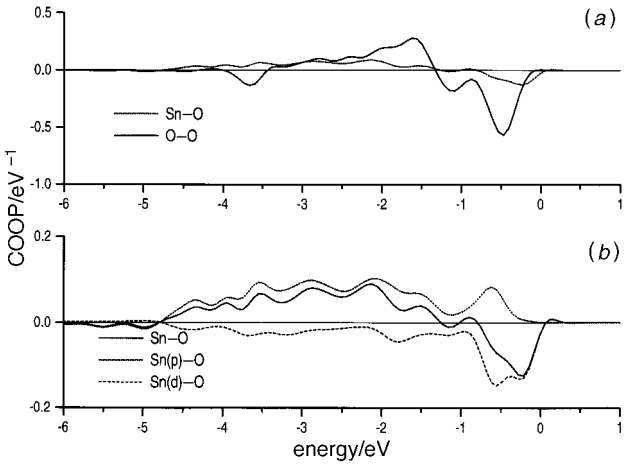

Fig. 3 Crystal orbital overlap population (COOP) for Sn—O and O—O interactions (*a*); tin l-projected COOP for Sn—O interactions (*b*)

interactions. Thus the upper part of the valence band is formed of antibonding Sn—O and O—O interactions. This can be more clearly observed when l-projected COOP are plotted. In Fig. 3(*b*), the Sn—O interaction is resolved for Sn(p) and Sn(d) contributions. This clearly shows that Sn(p)—O interaction is bonding up to the top of the valence band, this is because Sn(p)-states are filled with less than one electron so that all electrons coming from oxygen will be bonding. On the contrary because the Sn(d) band is nearly full all interactions with oxygen will be antibonding. The resulting COOP of Sn—O interaction is that the lower part of the valence band is bonding and the upper part antibonding as shown in Fig. 3(*a*).

UV absorption spectrum

The UV absorption spectrum of SnO_2 is calculated following the method described above for light polarized parallel to the tetragonal axis. Results are presented in Fig. 4. A shoulder is observed for photon energies right above the direct gap energy, *i.e.* 4.2 eV. This feature is due to transitions, from the O(p)-states in the valence band to Sn(s)-states in the conduction band, occurring at points located near the Γ-point in the Γ–M and Γ–Z directions of the BZ. A large number of direct transitions with a magnitude of *ca.* 8 eV is found to occur from O(p)-states to Sn(s)-states where the corresponding energy bands are relatively parallel, *i.e.* at the A-point and the M-point and near these points in the A–Z, A–M and M–Γ directions of the BZ. These transitions give rise to the peak observed at 8.0 eV and their initial states are lying in the strong O—O antibonding interaction region plotted in Fig. 3(*a*). The peak at 9.6 eV is probably due to transitions from the O(p)-states to Sn(s)-states occurring at the Z-point and the Γ-point and near these points in the Z–A, Γ–M and Γ–Z directions where numerous direct transitions of that magnitude are found. Another critical feature of the calculated absorption spectrum is a peak at 11.7 eV whose interpretation remains difficult due to a large number of transitions. However that peak seems to be mainly caused by transitions occurring all over the volume of the BZ investigated except the M–Γ zone where relatively few transitions of this magnitude are observed. Most of these transitions take place from the O(p)-states in the valence band to the Sn(p)-states in the conduction band but a significant amount of transitions with a magnitude of *ca.* 11.7 eV is also found to occur from O(p)-states to Sn(s)-states.

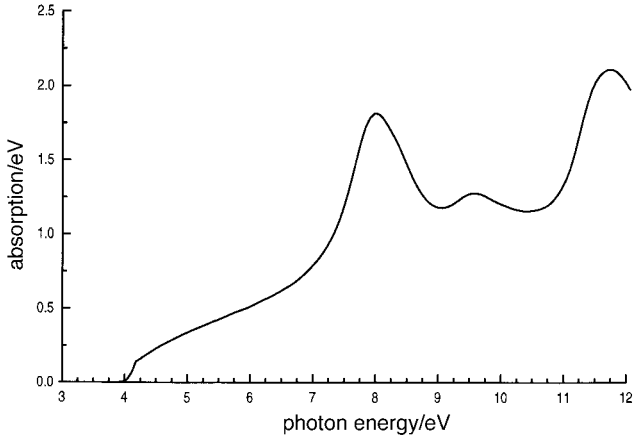

Fig. 4 UV absorption spectrum of SnO_2 for light polarization direction parallel to the tetragonal axis

In contrast to the character of the SnO_2 optical gap which has been intensively studied over the past decades, there are very few experimental data about the optical properties of SnO_2 for photon energies larger than the minimum band gap energy. Our results are found to agree with the shape of the reflectivity spectrum of SnO_2 measured by Jacquemin *et al.*[26] The peaks of the experimental reflectivity spectrum were observed at 4.3, 7.4, 8.9 and 10.9 eV, respectively, whereas our calculated absorption spectrum exhibits three peaks at 8.0, 9.6 and 11.7 eV, respectively, and a shoulder extending from 4.2 eV. The agreement between the two sets of results decreases as the photon energy increases, showing the degree of accuracy to be expected in the approach proposed here. Finally, it is of interest to note that experimentally it was found that the absorption of light polarized parallel to the tetragonal axis exhibits a diffuse edge around 3.95 eV,[27–30] which is in agreement with our calculations.

Conclusions

The augmented-spherical-wave (ASW) method used here within the density-functional theory (DFT) is found to provide a deeper understanding of the chemical bonding properties of SnO_2 since the crystal orbital overlap population (COOP) results show that the upper part of the valence band is formed by antibonding Sn(d)—O and O—O interactions combined with bonding Sn(p)—O interactions. Furthermore an overall agreement is found between the calculated and the experimental optical properties in the UV spectrum.

The calculations presented for the UV absorption spectrum were carried out with the ESOCS® program from Molecular Simulations, Inc.

References

1 K. Schwarz, *J. Phys. F : Met. Phys.*, 1986, **16**, L211.
2 S. F. Matar, G. Demazeau, J. Sticht, V. Eyert and J. Kübler, *J Phys. 1 Fr.*, 1992, **2**, 315.
3 P. I. Sorantin and K. Schwarz, *Inorg. Chem.*, 1992, **31**, 567.
4 S.-D. Mo and W. Y. Ching, *Phys. Rev. B*, 1995, **51**, 13 023.
5 J. L. Jacquemin, C. Alibert and G. Bordure, *Solid State Commun.*, 1972, **10**, 1295.
6 J. L. Jacquemin and G. Bordure, *J. Phys. Chem. Solids*, 1975, **36**, 1081.
7 F. J. Arlinghaus, *J. Phys. Chem. Solids*, 1974, **35**, 931.
8 J. Robertson, *J. Phys. C : Solid State Phys.*, 1979, **12**, 4767.
9 A. Svane and E. Antoncik, *J. Phys. Chem. Solids*, 1987, **48**, 171.
10 K. C. Mishra, K. H. Johnson and P. C. Schmidt, *Phys. Rev. B*, 1995, **51**, 13 972.
11 I. Manassidis, J. Goniakowski, L. N. Kantorovich and M. J. Gillan, *Surf. Sci.*, 1995, **339**, 258.
12 S. F. Matar, G. Demazeau, P. Mohn, V. Eyert and S. Najm, *Eur. J. Solid State Inorg. Chem.*, 1994, **31**, 615.
13 A. R. Williams, J. Kübler and C. D. Gelatt Jr., *Phys. Rev. B*, 1979, **19**, 6094.
14 W. Kohn and P. Vashishta, in *Theory of the inhomogeneous*

electron gas, ed. S. Lundquist and N. H. March, Plenum Press, New York, 1983, pp. 79–147.
15 J. von Barth and D. Hedin, *J. Phys. C*, 1972, **5**, 1629.
16 J. F. Janak, *Solid State Commun.*, 1978, **25**, 53.
17 R. Hoffmann, *Angew. Chem., Int. Ed. Engl.*, 1987, **26**, 846.
18 C. S. Wang and J. Callaway, *Phys. Rev. B*, 1974, **9**, 4897.
19 R. Kubo, *J. Phys. Soc. Jpn.*, 1957, **12**, 570.
20 R. W. G. Wyckoff, in *Crystal Structures*, 2nd edn., John Wiley & Sons Inc., New York, 1963, vol. 1, p. 250.
21 P. L. Gobby and G. J. Lapeyre in *Physics of semiconductors*, ed. F. G. Fumi, North-Holland, Amsterdam, 1976.
22 T. Arai, *J. Phys. Soc. Jpn.*, 1958, **15**, 916.
23 T. L. Credelle, C. G. Fonstad and R. H. Rediker, *Bull. Am. Phys. Soc.*, 1971, **16**, 519.
24 P. A. Cox, R. G. Egdell, C. Harding, W. R. Patterson and P. J. Tavener, *Surf. Sci.*, 1992, **123**, 179.
25 R. G. Egdell, W. R. Flavell and P. Tavener, *J. Solid State Chem.*, 1984, **51**, 345.
26 J. L. Jacquemin, C. Raisin and S. Robin-Kandare, *J. Phys. C: Solid State Phys.*, 1976, **9**, 593.
27 M. Nagasawa and S. Shionoya, *J. Phys. Soc. Jpn.*, 1971, **30**, 158.
28 R. Summitt, J. A. Morley and N. F. Borelli, *J. Phys. Chem. Solids*, 1964, **25**, 1465.
29 R. Summitt and N. F. Borelli, *J. Appl. Phys.*, 1967, **37**, 2200.
30 R. D. McRoberts, C. G. Fonstad and D. Hubert, *Phys. Rev. B*, 1974, **10**, 5213.

Paper 7/03813E; *Received* 2*nd June*, 1997